

# Experimental Investigation of Heat Transfer and Pressure Drop Performance of a Circular Tube with Coiled Wire Inserts

**Arvind A. Kapse**

M.V.P.S's K.B.T. College of Engineering, India  
kapse.arvind@kbtcoe.org (corresponding author)

**Vinod C. Shewale**

M.V.P.S's K.B.T. College of Engineering, India  
shewale.vinod@kbtcoe.org

**Sanjay D. Barahate**

K.K. Wagh Institute of Engineering Education & Research, India  
sdbarahate@kkwagh.edu.in

**Amol B. Kakade**

M.V.P.S's K.B.T. College of Engineering, India  
kakade.amol@kbtcoe.org

**Satish J. Surywanshi**

M.V.P.S's K.B.T. College of Engineering, India  
suryawanshi.satish@kbtcoe.org

Received: 21 October 2023 | Revised: 8 November 2023 and 24 November 2023 | Accepted: 26 November 2023

Licensed under a CC-BY 4.0 license | Copyright (c) by the authors | DOI: <https://doi.org/10.48084/etasr.6551>

## ABSTRACT

This paper evaluates the thermo-hydraulic performance of a coiled wire passive insert for internal turbulent flow through a circular copper tube test section in an in-tube exchanger. Experiments were carried out using water as the working fluid with Reynolds number ranging from 8000 to 32000. The experimental setup was validated for Nusselt number and friction factor with well-established equations for plain tubes. The average Nusselt number ratios ( $Nu_a/Nu_p$ ) and the friction factor ratios ( $f_a/f_p$ ) for the augmented tube case over the plain tube case are reported to range from 1.55 to 1.38 and from 1.513 to 1.583, respectively. The average performance ratios considering equal pumping power criteria are also reported and found in the range of 0.846 to 0.921. The study concludes that coiled wire inserts are suitable for heat transfer augmentation applications where pumping power is of minor concern.

*Keywords-passive insert; average performance ratio; turbulent flow*

## I. INTRODUCTION

Many engineering applications typically use heat exchangers. Numerous engineering methods have been developed during the past few decades to improve heat transfer in heat exchangers. Using tabulator components to ameliorate fluid turbulence and, consequently, the heat transfer coefficient from the flow surface, is one of these methods. This procedure has been widely used in various heat exchanger applications, including refrigeration, automotive, process industries, solar water heaters, etc. [1], since it has been shown to lower heat exchanger sizes while saving energy. In general, there are three

method categories for upgrading heat transfer: active methods, passive methods, and compound methods [1]. An active method improves heat transmission by utilizing some external power. A passive method deals with the insertion of tabulator elements into the tube while the compound technique involves the combination of active and passive methods together.

Authors in [2] reported the suitability of spring wire as a tabulator for spiral tube heat exchanger applicable for solar ponds. It was observed that spring tabulators either increase the heat transfer rate for a given length of spiral tube exchanger or reduce the heat exchanger size for the same rate of heat

transfer. Authors in [3] tested parallel-type and V-shaped vortex generators with rectangular blades and reported heat transfer and flow friction improvements that reached 568%. Authors in [4] tested coiled wires with square cross section in the Reynolds number range of 5000 to 25000 using air and recorded a rapid decrement in heat transfer augmentation when increasing Reynolds number. Authors in [5] reported the influence of wire coils which have convergent, convergent-divergent, and divergent shapes on heat transfer. This transfer is conducted through blending ethylene glycol with water of three different mixture volumes as a working fluid for Reynolds numbers from 4627 to 25,099. Both heat transfer and frictional resistance increased on all wire coils. Authors in [6] investigated the thermo-hydraulic performance of non-circular cross sectioned wire springs in spiral tube based heat exchangers. Triangular, square, rectangular, and hexagonal cross sections were. Authors in [7] measured the swirl flow heat transfer and pressure drop for water using helical coil wire with exponentially increasing heat input at different mass velocities. The authors also numerically solved the  $k-\epsilon$  turbulence model in a circular tube considering the temperature dependence of the thermophysical properties concerned. They derived the correlations for the swirl flow heat transfer in a vertical circular tube with helical coil wire. Authors in [8] carried out an experimental study to find the geometry effects of conical twisted strip inserts on the Nusselt number and friction coefficient. The study noted that Nusselt number and friction coefficient increased for all the inserted cases and decreased with a twist angle and a pitch ratio. Also, a greater Nusselt number increment was noticed at lower Reynolds numbers. Authors in [9] outlined the heat transfer and pressure drop performance of bakelite helical screw and hemispherical cup insert for individual and compound insertion in a tube in tube heat exchanger in the Reynolds number range of 8000-32000. The average performance ratios ( $Nu_a/Nu_c$ ) reported were in the range of 1.02 -1.11 for helical screw tape, 0.6 – 0.67 for cup shape insert, and 0.99 – 1.22 for two compound insertion cases based on equal pumping power criteria. Authors in [10] proposed a new turbulator called continuous cutting-edge helical lens insert. The experimental data of Nusselt number and friction coefficient were collected from the new turbulator using swirl ratios equal to 3 and 5. Based on the results, the authors suggested using the proposed input considering the higher heat transfer rate and acceptable pressure increase. Authors in [11] reviewed passive heat transfer augmentation techniques and highlighted their principles and thermo-hydraulic performance characteristics. Authors in [12] spotted monotonical increments in the Nusselt number with Reynolds number and number of swirls in their investigation of convergent pipe. The pipe was fitted with a pre swirl device at entry with air as a working medium between Reynolds numbers from 7970 to 47820. Authors in [13] optimized four independent parameters of coiled wire inserts i.e. thickness, length, pitch, and flow regime affecting heat transfer and pressure drop. Three experimental analysis techniques were employed by implementing the Taguchi experimental design method for parametric optimization. Authors in [14] discussed the effect of various baffle tabulators arrangement on heat transfer performance of a tube between Reynolds numbers 6000 and 20000. Among the selected types,

the heat enhancement along with the heat transfer enhancement factor were found to be maximum for twisted cross baffles arrangement. In contrast, minimum values were reported for the straight cross baffles arrangement. The highest thermal enhancement factor of 1.7 was documented for twisted cross baffles arrangement. Authors in [15] performed numerical analysis heat transfer improvement in a receiver tube of a solar collector engaging various materials and nanofluids while using Monte Carlo Ray Trace (MCRT) and CFD. Nanoparticles were utilized and thermal efficiency enhancement in the range of 3 to 14% was documented. In [16], numerical investigation was conducted to study the effect of a corrugated bottom wall on the heat transfer in a triangular solar collector. It was seen that the flow structure is sensitive to the Rayleigh number and that heat transfer is upgraded with this parameter increment. Authors in [17] investigated numerically two-dimensional natural convection heat and mass transfer generated in an inclined rectangular porous cavity filled with a Newtonian fluid. The authors measured heat and mass transfer rate in the cavity in terms of the average Nusselt and Sherwood numbers for various non-dimensional parameters. They presented the results in terms of streamlines, isotherms, and iso-concentrations.

Coil wires can be manufactured with simple processes and are easy for installation and removal in the tubes. Moreover, they do not cause sudden pressure drops or higher heat transfer enhancement but give better results at low Reynolds numbers. Due to their helical shape, the coiled wires introduce swirls in the flow resulting in better heat transfer rates. In the present investigation, the experimentally measured effects of coiled wire inserts on heat transfer and pressure drop in a circular tube are mentioned.

## II. EXPERIMENTAL SET UP AND METHODOLOGY

### A. Coiled Wire Insert Details

A steel coiled wire insert 0.8 m long with 18.2 mm diameter and 0.8 mm thickness is prepared for a full length insertion of the test section. The insert is shown in Figure 1.

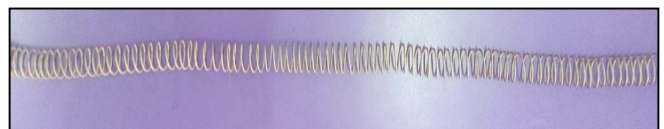


Fig. 1. A picture of the coiled wire insert.

### B. Arrangement of experimental set up

The experimental arrangement can be seen in [18]. Before the conduction of trials with inserts, plain tube results are required to be validated with well-established equations to gain confidence in the experimental work. Hence, trials are carried out initially on the plain tube for validation of the experimental set up for Reynolds number ranging from 8000 to 32000 with a step of 4000. After that, plain tube validation, trials are conducted for the inserted tube case. The procedure followed during conducting trials is:

The water was stored in a 100 L hot water tank equipped with five 2 kW heaters and was heated to a temperature of 75

°C. It was then circulated through the ring in a closed circuit with a hot water circulation pump. The hot water tank is deliberately kept 0.5 m above the hot water circulation pump to avoid the possibility of cavitation. A gate valve installed in the hot water circulation pipe maintains the necessary flow rate. The flow rate is calculated from the differential manometer reading of the U-tube manometer connected to a pre-calibrated Venturi meter. After that, cold water is fed counter currently from a large underground water tank through an inner tube (test section) of a cold water circulation pump in a closed circuit. The required flow rate is maintained in the cold water circulation line by one bypass valve and two shut-off valves. The cold water flow rate is calculated by measuring the differential pressure head with a manometer through a calibrated Venturi meter located in the cold water piping upstream of the test section. The pressure drop in the test section is measured by a U-tube manometer whose manometric liquid is carbon tetrachloride (CCl4). The system is then allowed to reach a steady state while temperature and pressure drop are measured for a plain tube at a cold water Reynolds number based on the test section inlet of 8000-32000.

All required temperatures are measured using pre-calibrated Copper/Constantan T-type thermocouples connected to a data logger. Cold and hot water temperatures are measured at the inlet and outlet points of the test section with two thermocouples placed at each location, whereas the average temperature is measured to improve accuracy. The outer surface wall temperature of the tube test section is measured by six thermocouples, which are placed around and equidistant from the surface. A complete photo of the experimental setup is shown in Figure 2.



Fig. 2. The actual set up.

C. Test Set Up Validation

Based on the data collected from the standard tube tests, the test setup is validated as described below:

$$Nu = 0.023Re_p^{0.8}Pr^{0.4} \text{ (Dittus Boelter)} \tag{1}$$

$$Nu = \frac{(f/8)(Re-1000)Pr}{1+12.7(f/8)^{1/2}(Pr^{2/3}-1)} \text{ (Gnielinski)} \tag{2}$$

$$f = 0.079Re^{-0.25} \text{ (Blasius)} \tag{3}$$

$$f = (0.79\ln Re - 1.64)^{-2} \text{ (Petukhov)} \tag{4}$$

A comparison of the experimental Nusselt number results and the friction coefficient of the above equations can be noticed in Figures 3 and 4 [19].

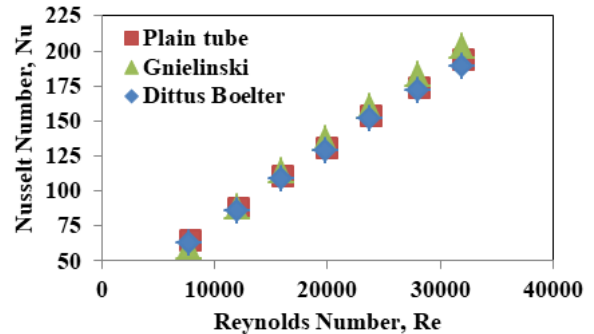


Fig. 3. Nusselt number for plain tube.

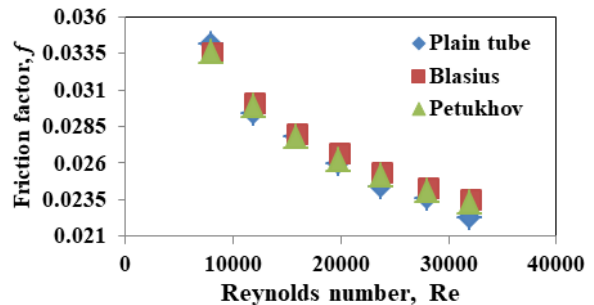


Fig. 4. Friction factor for plain tube.

It can be seen from the figures that the experimental results agree well with the above equations with deviations of 10% of the Nusselt number and 8% of the friction coefficient. Thus, the plain tube is verified and further test runs are conducted for different inserts.

D. Uncertainties in Measurements

The maximum uncertainties in measurements and non-dimensional parameters are shown in Tables I and II.

TABLE I. MAXIMUM MEASUREMENT UNCERTANTIES

Measuring parameter	Instrument	Uncertainty
Pressure	U-tube manometer	±1 mm of CCl4 column
Mass flow rate	Venturimeter	±0.0125 kg/s
Temperature	T-type thermocouple	±0.4 °C

TABLE II. MAXIMUM NON -DIMENSIONAL PARAMETER UNCERTANTIES

Non dimensional parameter	Maximum uncertainty
Reynolds number (Re)	±6.54%
Augmented tube Nusselt number (Nu <sub>a</sub> )	±8.85%
Equivalent Nusselt number (Nu <sub>e</sub> )	±10.82%
Friction factor	±12.67 %

III. ANALYSIS OF DATA

The collected temperature, pressure, and mass flow rate experimental data were analyzed for the performance

evaluation of the coil wire insert. The average Nusselt number and the friction coefficient are calculated from the inside diameter of the test piece. The thermal gain of cold water is obtained as follows:

$$Q_c = \dot{m}_c C_{p,w} (T_{c,out} - T_{c,in}) \quad (5)$$

The thermal loss of hot water in annulus is calculated as:

$$Q_h = \dot{m}_h C_{p,w} (T_{h,in} - T_{h,out}) \quad (6)$$

Due to the convection and radiation losses, the difference in heat gain between cold and hot water was found to be 3-10%. Thus, the average inner heat transfer coefficient ( $h_i$ ) is calculated based on the average heat transfer rate ( $Q_{avg}$ )

$$Q_{avg} = \frac{Q_c + Q_h}{2} \quad (7)$$

When calculating the average heat transfer coefficient of the inner side, it is assumed that the surface temperature of the tube wall is constant. Therefore, by neglecting the thermal resistance of the copper pipe wall, the heat transfer coefficient ( $h_i$ ) is calculated as follows [20]:

$$Q_{avg} = h_i A_i \Delta T_{lm} \quad (8)$$

where:

$$\Delta T_{lm} = \frac{(\bar{T}_s - T_{c,out}) - (\bar{T}_s - T_{c,in})}{\ln[(\bar{T}_s - T_{c,out}) / (\bar{T}_s - T_{c,in})]} \quad (9)$$

and:

$$A_i = \pi D_i L \quad (10)$$

The surface temperature of the tube wall is considered to be the average temperature of the ones recorded by the six thermocouples (test section) placed on the outer surface of the tube wall. ( $\bar{T}_s$ )

$$\bar{T}_s = \sum T_s / 6 \quad (11)$$

The average Nusselt number is obtained from the average heat transfer coefficient as:

$$Nu = \frac{h_i D_h}{k} \quad (12)$$

The average friction factor coefficient is calculated by:

$$f = \frac{\Delta P}{\left(\frac{L_1}{D_i}\right) \left(\frac{\rho V^2}{2}\right)} \quad (13)$$

where  $V$  is the average velocity of the working fluid in the inner tube. Thermophysical properties are measured at bulk mean average temperature of the liquid.

Authors in [21] suggested a set of 8 performance evaluation criteria (R1 to R8) to achieve these objectives. Performance evaluation criteria R1 and R3 were used in the present experimental work to determine heat transfer enhancement for different inserts. R1 corresponds to the ratio of augmented tube Nusselt number to the plain tube Nusselt number at the same Reynolds number. The average performance ratio (R3) is the ratio of the inserted tube Nusselt number to the plain tube Nusselt number corresponding to equal pumping power as it is

required for the inserted tube to maintain the flow. The performance ratio R3 is derived as follows [22]:

$$R_3 = \frac{Nu_a}{Nu_c} \quad (14)$$

The Nusselt number for the equivalent plain tube is calculated from the Dittus Boelter equation:

$$Nu_c = 0.023 Re_c^{0.8} Pr^{0.4} \quad (15)$$

where the equivalent Reynolds number is given by:

$$Re_c^{2.75} = f_a \times \frac{Re_a^3}{0.079} \quad (16)$$

where  $Nu_a$  is the Nusselt number of the tube with augmentation,  $Nu_p$  is the Nusselt number of the plain tube, and  $Nu_c$  is the Nusselt number of the plain tube at equivalent pumping power as that of the tube with augmentation.  $f_a$ ,  $f_p$ ,  $f_c$  are the friction factors of the above cases and  $Re_a$ ,  $Re_c$ , are the Reynolds numbers, respectively.

#### IV. RESULTS AND DISCUSSION

The inserted tube Nusselt numbers for the corresponding range of Reynolds numbers are found in the range of 98.83 to 269.7 as shown in Figure 5. The corresponding values for plain tube are ranging between 63.7 and 194. The Nusselt number increment is higher at higher values of Reynolds number. Thus, it may be concluded that the effect of coiled wire inserts on heat transfer enhancement increases at higher Reynolds number values. Due to their spiral shape, the twisted wires create vortices in the flow, resulting in better heat transfer rates. The impact of coiled wire insertion on the pressure drop in the test section is expressed in terms of friction factor in Figure 6.

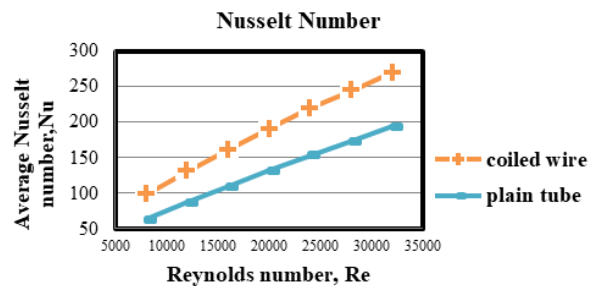


Fig. 5. Average Nusselt number Vs Reynolds number.

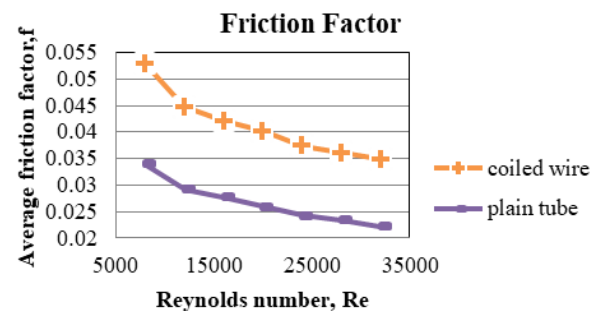


Fig. 6. Average friction factor Vs Reynolds number.

It is detected that the friction factor ranges from 0.0528 for Reynolds number equal to 8000 to 0.0349 for Reynolds number equal to 32000 for coiled wire. The coiled wire insert creates obstacles in the flow passage resulting in flow pressure drop in the test section for the coiled wire inserted tube.

The average Nusselt number ratios for the selected range of Reynolds numbers are shown in Figure 7. The Nusselt number increment ranges from 1.55 to 1.38 for Reynolds number values from 8000 to 32000 respectively. This shows that the heat transfer improvement reduces with increasing Reynolds number due to the weak laminar sub layer breaking caused at higher mass flow rates. The laminar sub layer breaking is expected to be promoted by the wire surface near the tube wall resulting in higher heat transfer rates which might be effective at low Reynolds numbers.

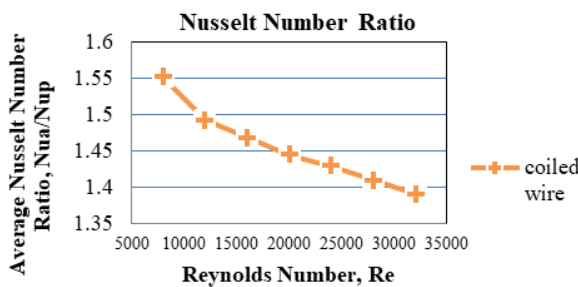


Fig. 7. Average Nusselt number ratio Vs Reynolds number.

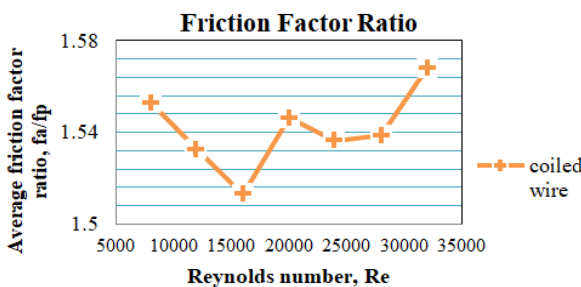


Fig. 8. Average friction factor ratio Vs Reynolds number.

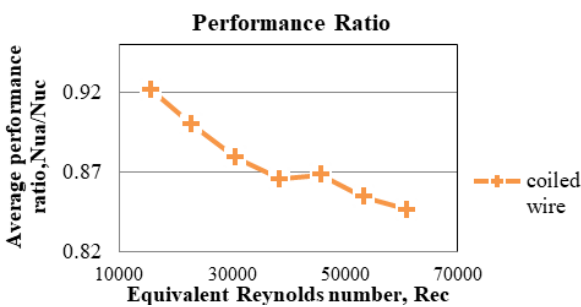


Fig. 9. Average performance ratio Vs equivalent Reynolds number.

Average friction factor ratios for the selected range of Reynolds numbers are shown in Figure 8. The increment in the friction factor ranges from 1.513 to 1.583 for Reynolds numbers from 8000 to 32000. It is seen that the flow friction fluctuates with Reynolds number and tends to increase the pumping power requirements at higher Reynolds number. The

thermo hydraulic performance of the insert in terms of performance ratio R3 is shown in Figure 9.

Performance ratio ranges between 0.921 and 0.846 for Reynolds numbers from 8000 to 32000. It is seen that R3 is less than 1 for the selected range of Reynolds number values of this study. Also, the performance ratio decreases at higher Reynolds numbers. Although the enhancement in Nusselt number is seen for the selected Reynolds number range, friction factor increments are also considerable. Looking into the increased pumping power requirements and the observed range of performance ratios, the thermo hydraulic performance of the insert is not competitive in the selected Reynolds number range.

V. CONCLUSIONS

The thermo hydraulic performance of coiled wire for turbulent flow is evaluated in the Reynolds number range of 8000-32000. The experimental investigation reveals that the coiled wire inserts introduce swirl in the flow due to their helical shape resulting in better heat transfer rates. However, the frictional resistance also increases demanding higher pumping power requirements. A thermo hydraulic performance indicator R3, was observed to be less than unity for the selected range of Reynolds numbers. This indicates that the coiled wire inserts are suitable for heat transfer augmentation in applications where pumping power requirements are not a major concern.

ACKNOWLEDGMENT

The authors would like to express their gratitude to Dr. S.V. Kasar, Dr. P.W.Deshmukh, and Dr.S.B.Sonawane for providing insight and expertise which contributed greatly to this research.

ABBREVIATIONS AND ACRONYMS

A	-	Area [m <sup>2</sup> ]
D	-	Diameter [m]
$\Delta P$	-	Pressure drop of fluid [Nm <sup>-2</sup> ]
$\Delta T_{lm}$	-	Logarithmic mean temperature difference [°C]
h	-	Heat transfer coefficient [Wm <sup>-2</sup> K <sup>-1</sup> ]
k	-	Thermal conductivity [Wm <sup>-1</sup> K <sup>-1</sup> ]
l	-	Length of insert [m]
L	-	Length of test section for heat transfer [m]
L1	-	Length of tube between pressure taps [m]
m'	-	Mass flow rate of fluid [kgsec <sup>-1</sup> ]
Q	-	Heat transfer rate [kW]
T	-	Temperature [°C]
V	-	Mean fluid velocity [msec <sup>-1</sup> ]
C <sub>pw</sub>	-	Specific heat at constant pressure [kJkg <sup>-1</sup> K]
Re	-	Reynolds number (=ρVD/μ) [-]
R3	-	Average performance ratio [-]
Pr	-	Prandtl number (=μC <sub>p</sub> /k) [-]
ρ	-	Fluid density [kgm <sup>-3</sup> ]
μ	-	dynamic viscosity [kgms <sup>-1</sup> ]
Subscripts		
a	-	Augmented tube case
avg	-	Average
c	-	Cold
h	-	Hot
i	-	Inner
in	-	Inlet
o	-	Outer
out	-	Outlet
p	-	Plain tube case
s	-	Tube wall surface

## REFERENCES

- [1] S. Liu and M. Sakr, "A comprehensive review on passive heat transfer enhancements in pipe exchangers," *Renewable and Sustainable Energy Reviews*, vol. 19, pp. 64–81, Mar. 2013, <https://doi.org/10.1016/j.rser.2012.11.021>.
- [2] F. Aldawi, "Proposing the employment of spring-wire turbulator for flat spiral tubes utilized in solar ponds, experimental study," *Case Studies in Thermal Engineering*, vol. 36, Aug. 2022, Art. no. 102180, <https://doi.org/10.1016/j.csite.2022.102180>.
- [3] K. Zhang, Z. Sun, N. Zheng, and Q. Chen, "Effects of the configuration of winglet vortex generators on turbulent heat transfer enhancement in circular tubes," *International Journal of Heat and Mass Transfer*, vol. 157, Aug. 2020, Art. no. 119928, <https://doi.org/10.1016/j.ijheatmasstransfer.2020.119928>.
- [4] P. Promvong, "Thermal performance in circular tube fitted with coiled square wires," *Energy Conversion and Management*, vol. 49, no. 5, pp. 980–987, May 2008, <https://doi.org/10.1016/j.enconman.2007.10.005>.
- [5] O. Keklikcioglu and V. Ozceyhan, "Heat transfer augmentation in a tube with conical wire coils using a mixture of ethylene glycol/water as a fluid," *International Journal of Thermal Sciences*, vol. 171, Jan. 2022, Art. no. 107204, <https://doi.org/10.1016/j.ijthermalsci.2021.107204>.
- [6] H. Moria, "A comprehensive geometric investigation of non-circular cross section spring-wire turbulator through the spiral-tube based heat exchangers," *Results in Engineering*, vol. 17, Mar. 2023, Art. no. 100906, <https://doi.org/10.1016/j.rineng.2023.100906>.
- [7] K. Hata and M. Shibahara, "Helically-coiled-wire-induced swirl flow heat transfer and pressure drop in a circular tube under velocities controlled," *International Journal of Heat and Mass Transfer*, vol. 204, May 2023, Art. no. 123849, <https://doi.org/10.1016/j.ijheatmasstransfer.2023.123849>.
- [8] M. Bahiraei, K. Gharagozloo, and H. Moayedi, "Experimental study on effect of employing twisted conical strip inserts on thermohydraulic performance considering geometrical parameters," *International Journal of Thermal Sciences*, vol. 149, Mar. 2020, Art. no. 106178, <https://doi.org/10.1016/j.ijthermalsci.2019.106178>.
- [9] A. A. Kapse, V. C. Shewale, and S. P. Mogal, "Evaluation of Thermo hydraulic Performance of Passive and Compound Inserts," *Journal of Applied Science and Engineering*, vol. 27, no. 1, pp. 1877–1887, 2023, [https://doi.org/10.6180/jase.202401\\_27\(1\).0004](https://doi.org/10.6180/jase.202401_27(1).0004).
- [10] R. M. Sarviya and V. Fuskele, "Heat Transfer and Pressure Drop in a Circular Tube Fitted with Twisted Tape Insert Having Continuous Cut Edges," *Journal of Energy Storage*, vol. 19, pp. 10–14, Oct. 2018, <https://doi.org/10.1016/j.est.2018.07.001>.
- [11] S. Liu and M. Sakr, "A comprehensive review on passive heat transfer enhancements in pipe exchangers," *Renewable and Sustainable Energy Reviews*, vol. 19, pp. 64–81, Mar. 2013, <https://doi.org/10.1016/j.rser.2012.11.021>.
- [12] C. S. Yang, D. Z. Jeng, Y.-J. Yang, H.-R. Chen, and C. Gau, "Experimental study of pre-swirl flow effect on the heat transfer process in the entry region of a convergent pipe," *Experimental Thermal and Fluid Science*, vol. 35, no. 1, pp. 73–81, Jan. 2011, <https://doi.org/10.1016/j.expthermflusci.2010.08.008>.
- [13] S. Kapan, N. Celik, E. Turgut, and V. Tanyildizi, "A comprehensive optimization and design analysis of a heat exchanger with coiled wire turbulators," *Heat and Mass Transfer*, vol. 59, no. 8, pp. 1507–1524, Aug. 2023, <https://doi.org/10.1007/s00231-023-03348-w>.
- [14] K. Nanan, C. Thianpong, M. Pimsarn, V. Chuwattanakul, and S. Eiamsa-ard, "Flow and thermal mechanisms in a heat exchanger tube inserted with twisted cross-baffle turbulators," *Applied Thermal Engineering*, vol. 114, pp. 130–147, Mar. 2017, <https://doi.org/10.1016/j.applthermaleng.2016.11.153>.
- [15] D. Guerraiche, K. Guerraiche, Z. Driss, A. Chibani, S. Merouani, and C. Bougriou, "Heat Transfer Enhancement in a Receiver Tube of Solar Collector Using Various Materials and Nanofluids," *Engineering, Technology & Applied Science Research*, vol. 12, no. 5, pp. 9282–9294, Oct. 2022, <https://doi.org/10.48084/etasr.5214>.
- [16] W. Aich, "3D Buoyancy Induced Heat Transfer in Triangular Solar Collector Having a Corrugated Bottom Wall," *Engineering, Technology & Applied Science Research*, vol. 8, no. 2, pp. 2651–2655, Apr. 2018, <https://doi.org/10.48084/etasr.1857>.
- [17] A. Latreche and M. Djezzar, "Numerical Study of Natural Convective Heat and Mass Transfer in an Inclined Porous Media," *Engineering, Technology & Applied Science Research*, vol. 8, no. 4, pp. 3223–3227, Aug. 2018, <https://doi.org/10.48084/etasr.2179>.
- [18] A. A. Kapse, P. R. Dongarwar, and R. R. Gawande, "Thermohydraulic performance comparison of compound inserts for a turbulent flow through a circular tube," *Thermal Science*, vol. 21, no. 3, pp. 1309–1319, 2017, <https://doi.org/10.2298/TSCI151027096K>.
- [19] A. A. Kapse, P. R. Dongarwar, and R. R. Gawande, "Experimental investigation of turbulent heat transfer performance in internal flow using a star shape cross sectioned twisted rod inserts," *Heat and Mass Transfer*, vol. 53, no. 1, pp. 253–264, Jan. 2017, <https://doi.org/10.1007/s00231-016-1820-7>.
- [20] F. P. Incropera, D. P. DeWitt, T. L. Bergman, and A. S. Lavine, *Fundamentals of Heat and Mass Transfer*, 6th ed. Hoboken, NJ, USA: John Wiley & Sons, 2006.
- [21] V. D. Zimparov and N. L. Vulchanov, "Performance evaluation criteria for enhanced heat transfer surfaces," *International Journal of Heat and Mass Transfer*, vol. 37, no. 12, pp. 1807–1816, Aug. 1994, [https://doi.org/10.1016/0017-9310\(94\)90069-8](https://doi.org/10.1016/0017-9310(94)90069-8).
- [22] P. W. Deshmukh and R. P. Vedula, "Heat transfer and friction factor characteristics of turbulent flow through a circular tube fitted with vortex generator inserts," *International Journal of Heat and Mass Transfer*, vol. 79, pp. 551–560, Dec. 2014, <https://doi.org/10.1016/j.ijheatmasstransfer.2014.08.042>.